Hydroxyl Radical and Hydroxide Ion in Liquid Water: A Comparative Electron Density Functional Theory Study

Peter Vassilev,* Manuel J. Louwerse, and Evert Jan Baerends*

Divisie Scheikunde, afd. Theoretische Chemie, Vrije Universiteit Amsterdam, De Boelelaan 1083, Amsterdam 1081 HV, The Netherlands

Received: November 17, 2004; In Final Form: August 15, 2005

Ab initio density functional theory molecular dynamics simulations of the solvated states of the hydroxyl radical and hydroxide ion are performed using the Becke−Lee−Yang−Parr (BLYP) exchange-correlation functional (Becke, A. D. *Phys. Rev. A* **1988**, *38*, 3098. Lee, C.; Yang, W.; Parr, R. G. *Phys. Rev. B* **1988**, *37*, 785). The structures of the solvation shells of the two species are examined. It is found that the OH radical forms a relatively well-defined solvation complex with four neighboring water molecules. Three of these molecules are hydrogen bonded to the OH, while the fourth is hemibonded via a three-electron two-centered bond between the oxygen atoms of the OH and water. The activity and the diffusion mechanism of the OH radical in water is discussed in comparison with the OH^- ion. Although the results are partially influenced by the tendency of the BLYP density functional to overestimate hemibonded structure, the present simulations suggest that the widely accepted picture of rapid diffusion of OH radical in water through hydrogen exchange reaction may need to be reconsidered.

Introduction

The hydroxyl radical in general and its hydrated state in particular is an important entity playing a major role in numerous biochemical, electrochemical, and atmospheric reactions. As a derivative of the hydroxide peroxide, $OH^\bullet$ is also a powerful oxidizing and bleaching agent with an industrial application. The formation and presence of $OH^\bullet$ in biological cells is recognized as the cause of numerous cell diseases (see, for example, ref 1 and references therein). As an intermediate, the $OH^\bullet$ radical is believed to be of importance for many oxidation reactions as well as for the Fenton-like reactions,[2] although recently the latter assumption has been questioned on the basis of ab initio density functional theory results.[3,4]

The majority of these processes occur in liquid water or, as in the case of the earth's atmosphere, in liquid water droplets. The structure and the transport properties of the hydroxyl radical in water are decisive then for the kinetics of these reactions, and detailed knowledge of the solvation shell and bonding with the hydrating water molecules is vital for understanding the mechanism of these processes.

Several computational studies at different levels of the theory have investigated the $OH^\bullet$ radical and the formation of $OH^\bullet\cdot(H_2O)_n$ clusters,[1,5−12] but only a few have also considered the hydrated hydroxyl radical in liquid water.[1,9] The latter simulations of the solvated state, however, were performed using classical or hybrid solvation model methods.

With the development of the density functional theory[13,14] (DFT) and the Car−Parrinello[15] approach in particular, it became feasible to perform computer simulations of relatively small (but still representative for the real systems) computational models. One of the first subjects under study was liquid water.[16−19] The successful application of this computational scheme to reproduce and predict the experimentally observed data proved the applicability and efficiency of the DFT-based molecular dynamics (MD), and now an increasing number of publications are based on the same approach.

The hydronium H_3O^+ and the hydroxide OH^- ions have also been intensively studied.[20−24] It was shown that both H_3O^+ and OH^- introduce the so-called charge defect within the hydrogen-bond network of liquid water and display anomalously high mobilities realized via a proton-exchange reaction with a neighboring water molecule. This is also known as "structural diffusion".

Being a radical, the $OH^\bullet$ is generally recognized as a highly active species, and it is widely anticipated that the hydroxyl radical would also rapidly diffuse in liquid water via a *hydrogen* exchange reaction, analogously to the proton-exchange reaction in the case of the H_3O^+ and OH^- ions:

$$OH^\bullet + H_2O \rightarrow H_2O + OH^\bullet$$

The processes of proton or hydrogen exchange involve the breaking and formation of the rather strong internal O−H bond of the water molecule in a complex interplay with the much weaker hydrogen bonds governing the structure of the solvent. For this kind of system, the DFT-based ab initio molecular dynamics simulations have proven to be an invaluable tool and today also perhaps the only applicable method capable of producing enough statistical data in a reasonable amount of computational time.

Despite the importance of the hydroxyl radical in liquid water, to the best of our knowledge so far there have been no published ab initio molecular dynamics simulations of the hydrated $OH^\bullet$. The previous theoretical studies[1,9] were performed using classical MD or hybrid solvation models, and no structural information for the hydration complex of the $OH^\bullet$ was provided. The

* To whom correspondence should be addressed. E-mail: (P.V.) vassilev@few.vu.nl; (M.J.L.) louwerse@few.vu.nl; (E.J.B.) baerends@few.vu.nl.

10.1021/jp044751p CCC: $30.25
Published on Web 11/15/2005

$OH^{\bullet}\cdot(H_2O)_n$ complexes have been studied in detail using DFT and high-level ab initio methods.[1,5−12] It was shown that the hydroxyl radical can take part in hydrogen bonds with water molecules as either H-bond acceptor or through its own hydrogen atom as H-bond donor. Comparing DFT results using the BLYP exchange-correlation density functional proposed by Becke[25] and Lee et al.[26] with those of high-level ab initio methods, it was concluded that the BLYP functional also erroneously favors the formation of a direct (hemi-)bond between the oxygen of the $OH^{\bullet}$ and the oxygen of a neighboring water molecule.[1] A similar type of interaction, the so-called two-centered three-electron hemibond, was also found for other open-shell systems with a single unpaired electron.[27,28] The strength of the interaction was again overestimated by the BLYP functional compared to the post-Hartree−Fock results, and these findings put forward the question if the BLYP density functional can be used for these systems and for the hydrated $OH^{\bullet}$ in particular. Nevertheless, Hamad et al.[1] reported that for $OH^{\bullet}\cdot(H_2O)_n$ clusters, $n = 1,2, ..., 5$, the differences between the BLYP-DFT and post-Hartree−Fock MP2 simulations vanish with the increase of the number of complexing water molecules n. This indicates that despite the overestimated hemibond interaction, the BLYP density functional, which was proven to be one of the best for liquid water,[17] may still be suitable for MD simulations of $OH^{\bullet}$ in liquid water.

In this paper, we present an DFT-based ab initio molecular dynamics study of the hydrated $OH^{\bullet}$ using the BLYP exchange-correlation density functional. We will concentrate on the structural, dynamical, and electronic properties of the hydroxyl radical $OH^{\bullet}$ in comparison with the hydroxide ion OH^-. In the following analysis of the simulation data, O* will denote the oxygen center of the $OH^{\bullet}$ or OH^- as appropriate. To locate the OH species, all hydrogen atoms are assigned to the closest oxygen atom, and the oxygen to which just one H atom has been assigned is selected as being the one of $OH^{\bullet}$ or OH^-.

Computational Details

The molecular dynamics (MD) simulations were performed using the Car−Parrinello[15] density functional theory[13,14] package PAW implementing the projector augmented-wave method.[29] We used the BLYP exchange-correlation density functional.[25,26]

The computational models consist of (i) 32 water molecules (spin-restricted calculation), (ii) 31 water molecules and one OH^- species (total charge of −1, spin-restricted calculation), and (iii) 31 water molecules and one $OH^{\bullet}$ species (spin-polarized calculation) for the (i) pure liquid water, (ii) hydrated OH^-, and (iii) hydrated $OH^{\bullet}$ MD simulations. The size of the periodic cubic box in all three cases was 9.865 Å. The starting configurations for the hydroxyl radical and hydroxide ion simulations were prepared using a configuration taken from the pure liquid water simulation and taking away a hydrogen atom or a proton, respectively. The MD time step was 0.157 fs (6.5 au), and the fictitious mass for the electronic degrees of freedom was 100 au. The simulation lengths were 2ps, 15ps, and 32ps, respectively, for (i), (ii), and (iii). NVE molecular dynamics was performed for liquid water at a mean temperature $T = 291$ K (i); for the hydroxide ion (ii) and hydroxyl radical (iii) simulations the temperature was set to $T = 300$ K, controlled by a thermostat on the ionic degrees of freedom with an oscillation period of 30000 au (approximately 0.7ps) and 60000 au, respectively, for (ii) and (iii). Additionally frictions of 0.0004 and 0.001 for (ii) and (iii) were applied on the Nosé variable, and 0.00005 in either (ii) and (iii) on the electron wave function, as defined in the PAW code. To decrease the coupling between the electronic and ionic degrees of freedom, for the hydrogen atoms we used the deuterium isotope.

The cutoffs for the plane wave basis for the electron pseudowave function and the pseudocharge density were 408 eV (30 Ry) and 1225 eV (90 Ry), respectively. We used one s-projector for the H atoms and one s- and two p-projectors for the O atoms with only the valence electrons included in the calculation. For the construction of the H projector we used partial wave energy of $E = -0.24001$H and a radius of $R_c = 0.557$ au, as defined in the PAW atomic setups generation program. For the O atom, we used $E = -0.87577$H for the s-projector and $E = -0.33159$H and 0.27777H for the p-projectors with $R_c = 1.267$ au. This set of parameters, including the fictitious mass and the time step for the MD, were tested for liquid water and can produce a stable NVE MD simulation conserving the total energy within less than 0.005H for 2 ps. For the radial distribution functions we used a bin size of 0.04 Å. The projection scheme for calculating the projected density of states is based on the set of PAW projectors as implemented in the program PAW.

Results and Discussion

The ab initio molecular dynamics (MD) simulations of the hydrated states of $OH^{\bullet}$ and OH^- reveal that although the difference is "just" one electron, the two systems display rather dissimilar and in the case of $OH^{\bullet}$ unexpected structural and dynamical properties. The most appealing result was the lack of hydrogen exchange in the case of the radical. Contrary to the generally accepted picture for highly active $OH^{\bullet}$ species, we did not observe even a single hydrogen jump between the $OH^{\bullet}$ and the hydrating water molecules during the MD simulation of a length of 32 ps. This suggests that the widespread anticipation for rapid diffusion of the $OH^{\bullet}$ via a hydrogen exchange reaction with the surrounding water molecules may need to be reconsidered.

The origins of this behavior are in the specific structural characteristics of the solvation shells of the radical. The goal of this paper is to give a detailed description of the solvation complex of hydroxyl radical in comparison with the hydroxide ion as found from the MD simulation. We will first look into the distribution functions characterizing the solvated states of the OH^- and $OH^{\bullet}$, and we will continue examining the electronic structure of the hydrated $OH^{\bullet}$. Finally, the oxidative properties and the diffusion mechanism of the OH radical in water are discussed.

Radial Distribution Functions. The comparison between the O*- -O radial distribution functions (RDF) of the hydroxyl radical and hydroxide ion, O* being the oxygen atom from OH, reveals that in both cases the coordination shells are characterized with a major peak at around 2.75 and 2.6 Å for $OH^{\bullet}$ and OH^-, respectively (Figure 1). The integrated values of the RDFs up to the minimum at ca. 3 Å is in either case around four, i.e., at first approximation four water molecules constitute the coordination shell of the two species. However, in the case of the radical there is an additional peak at around 2.3 Å with an integrated value of one, which indicates the presence of one water molecule in a rather close contact with the central $OH^{\bullet}$. The distance of 2.3 Å is much shorter than the O- -O separation of around 2.8 Å for a hydrogen bond. Neither liquid water nor the hydroxide ion exhibit a similar peak in their RDFs and this suggests that the first coordination shell of the $OH^{\bullet}$ has a rather different and unique composition. However, the O- -O radial distribution function alone does not provide sufficient information to resolve the origin of this peak and to determine in detail

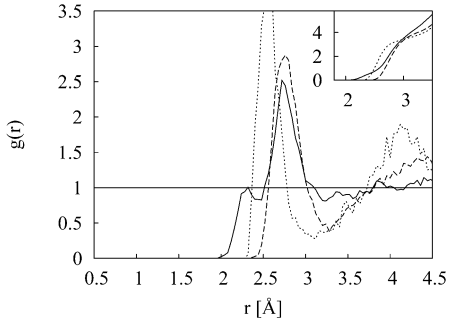

Figure 1. Oxygen−oxygen radial distribution functions (RDF): O*- -O RDF of hydroxyl radical (solid line), O*- -O RDF of hydroxide ion (dotted line), and O- -O RDF of pure liquid water (dashed line). O* denotes the oxygen atom from the OH species; O denotes the oxygen atoms from the water molecules. The integrated RDFs are given in the inset graph.

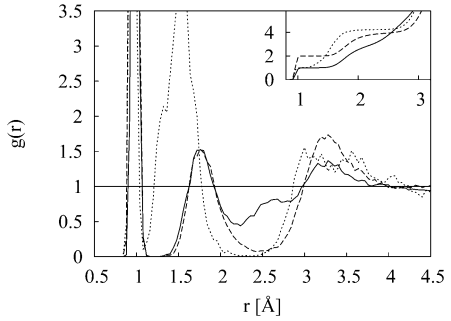

Figure 2. Oxygen−hydrogen radial distribution functions (RDF): O*- -H RDF of hydroxyl radical (solid line), O*- -H RDF of hydroxide ion (dotted line), and O- -H RDF of pure liquid water (dashed line). O* denotes the oxygen atom from the OH species, O denotes the oxygen atoms from the water molecules, and H denotes hydrogen atoms regardless of if they are from the OH species or water molecules. The integrated RDFs are given in the inset graph.

the structure of the $OH^{\bullet}\cdot(H_2O)_4$ hydration complex. A more thorough analysis of the simulation data is required, and such an analysis is presented later in this article introducing two-dimensional distribution functions.

From the oxygen−hydrogen RDFs it is noticeable that at short distances (Figure 2, $r < 2$ Å) the distribution function corresponding to the hydroxyl radical is comparable to the one of pure water. This suggests that analogous to H_2O, the $OH^{\bullet}$ itself is hydrogen-bonded with *at least* two of the four hydrating water molecules, as indicated from the integrated values of the peak in the O*- -H RDF at around 1.8 Å. However, an additional feature of the radical, which just as in the case of the O- -O distribution function cannot be explained only from the RDFs, is the presence of a peak at around 2.5 Å. We will come back to these data later in this paper.

Considering the second coordination shells (Figure 1, $r > 3-3.5$ Å), while they can be easily identified in the case of OH^- and H_2O, for the $OH^{\bullet}$ the radial distribution function approaches the unity value. This is equivalent to a random distribution of the water molecules with respect to the $OH^{\bullet}\cdot(H_2O)_4$ hydration complex itself, suggesting that the presence of $OH^{\bullet}$ results in a disruption of the hydrogen bonding network of liquid H_2O, and the radical cannot be considered as being embedded in the structure of water, as for example OH^- is. Quite the contrary, the hydroxide ion appears strongly bound to the hydrating water molecules leading to shortened O- -O and O- -H separations in the first coordination shell and enhanced structure of the solvent, reflected in the relatively more pronounced peaks in the distribution functions, especially the O*- -O RDF.

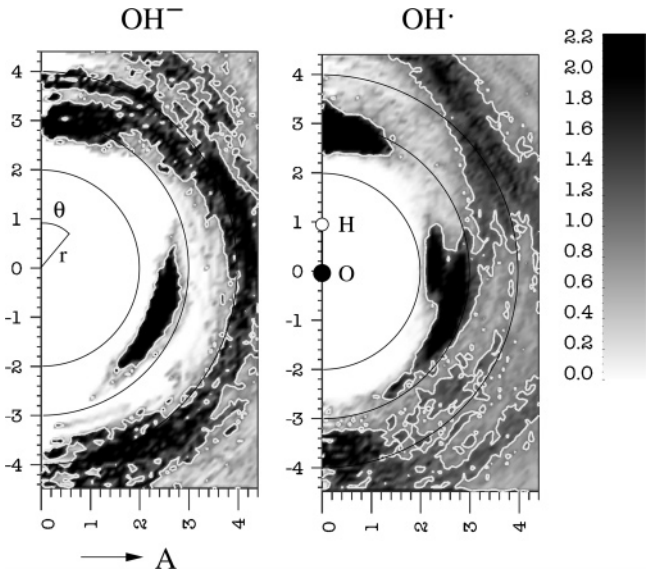

Figure 3. OH- -O distribution function $P(r,\theta)$ for the hydroxide ion (left panel) and hydroxyl radical (right panel). The single white isoline has a value of 1.0. See also the text.

Detailed Structure of the Solvation Complexes of OH^- and $OH^{\bullet}$. For the purpose of characterizing the solvation shells of the OH species we employ a two-dimensional OH- -X distribution function $P(r,\theta)$, where r is the distance between the oxygen atom O* of the hydroxyl radical and an atom of interest X, X being either O or H from the solvent (see also Figure 3). θ is the angle H*- -O*- -X, with H* being the hydrogen atom from the OH. The OH species is then along the vertical axes ($\theta = 0$) with the oxygen atom O* in the origin of the graph. For example, in the case of the OH^- in liquid water (left panel of Figure 3), the two-dimensional OH- -O radial distribution function shows a rather broad peak around $r = 2.6-2.7$ Å and θ in the range of $90-120°$, corresponding to the O atoms from the first coordination shell. Additionally, there is a peak at around $r = 3$ Å and $\theta = 0°$.

The structure of the hydrated OH^- has been determined previously by Tuckerman et al.[23] and therefore will not be discussed here. We will only recall that one can distinguish between two solvation states of the OH^-. The first one is characterized with four water molecules in the equatorial plane of the OH^- with the hydroxide ion being acceptor of the H-bonds. An additional fifth water molecule, which is further away and weakly bound with its O to the H atom of the OH^- ($\theta = 0$), was also found.[23] This complex was identified as the inactive state of the OH^- with respect to the proton exchange reaction with a neighboring H_2O. The second solvation complex is characterized with a tetrahedral configuration of the solvating H_2O, i.e., with three neighboring water molecules at θ around 120° as H-bond donors and a fourth water molecule acting as H-bond acceptor in a hydrogen bond with the H of OH^-. This complex was determined to be the active state for the proton-transfer reaction leading to the diffusion of the ion. In the course of this process the two states transform from one to the other.[23]

Without carrying out a full analysis of the simulation data as proposed by Tuckerman et al.,[23] we conclude that the current two-dimensional (2D) distribution function corroborates these previous findings. The broad distribution peak at $r = 2.6-2.7$ Å and θ in the order of $90-120°$ agrees well with the two solvation states of OH^-. The water molecules accounting for

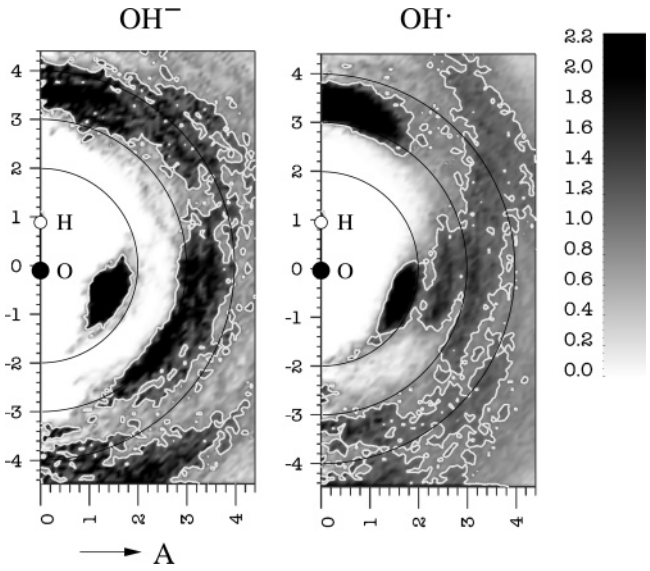

Figure 4. OH- -H distribution function $P(r,\theta)$ for the hydroxide ion (left panel) and hydroxyl radical (right panel). The single white isoline has a value of 1.0. See also the text.

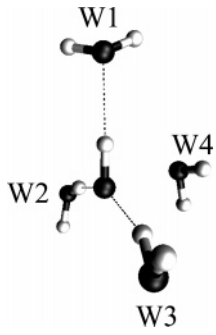

Figure 5. $OH^{\bullet}\cdot(H_2O)_4$ hydration complex in liquid water. The $OH^{\bullet}$ radical and the oxygen atoms from W1, W2, and W3 water molecules are approximately in one plane. See also the text.

this peak are H-bond donors for the OH^-, which can also be seen in the 2D OH—H distribution function representing the hydrogen atoms distribution around the central OH species (left panel in Figure 4). The peak at around $r = 1.5$ Å and $\theta = 90-120°$ represents the corresponding hydrogen atoms. The distance of $r = 1.5$ Å is shorter than the O*—O distance, meaning that the OH bonds point toward the O* center.

The 2D distribution function used in this work also shows the formation of the elongated hydrogen bond with the OH^- being H-donor, as already suggested in ref 23. The corresponding oxygen atom of the water molecule appears as a peak in the 2D distribution function at separation distances r on the order of 3 Å and $\theta = 0-20°$. Using a one-dimensional RDF, i.e., after integration over θ, this feature of the solvation shell would be undetectable (compare Figure 1 at $r = 3$ Å).

Considering the hydroxyl radical, being a *H-bond acceptor* analogous to the hydroxide ion, it forms hydrogen bonds with the neighboring water molecules (right panel in Figure 3, the broad peak at $r = 2.8$ Å, θ in the order of 90−120°). However, the peak in the distribution function only integrates to two, i.e., only two water molecules instead of the three to four found in the case of OH^-. As opposed to the hydroxide ion, the hydroxyl radical as a *H-bond donor* forms a strong hydrogen bond with a third water molecule, accounting for the well-pronounced peak at around $r = 2.8$ Å and $\theta = 0°$ (see also Figure 5). In the original one-dimensional O—O RDF (Figure 1), these three water molecules account for the single peak at around 2.8 Å. The additional peak at 2.3 Å is now easily recognizable in the 2D distribution function at $\theta = 90°$. The water molecule accounting for this peak is *not hydrogen bonded* to the $OH^{\bullet}$, and its hydrogen atoms account for the additional features around $r = 2.5$ Å with relatively broad distribution around $\theta = 90°$ in the OH−H 2D distribution function (Figure 4).

Thus, the structure of the $OH^{\bullet}\cdot(H_2O)_4$ solvation complex can be illustrated in Figure 5 with the three (W1, W2, W3) water molecules being hydrogen bonded and the "additional" (W4) water molecule in close contact with the $OH^{\bullet}$. It can also be shown, that the O* and the H* atoms of the $OH^{\bullet}$ and the three oxygen atoms from W1, W2, and W3 are approximately in one plane. The connection line between O* and the oxygen atom from W4 is then perpendicular to this plane.

The $OH^{\bullet}\cdot(H_2O)_4$ solvation complex displays rather different structural characteristics compared to the usual tetrahedral configuration of H_2O in liquid water and is rather stable in the course of the ab initio MD simulation (throughout the course of our 32 ps simulation the same four water molecules form the first coordination shell). As already mentioned above, its formation causes disruption in the arrangement of liquid water. While the $OH^{\bullet}\cdot(H_2O)_4$ is internally well structured, it forms rather weak hydrogen bonds with the surrounding solvent molecules. Although the finite box size may have an effect on these results for the second solvation shell, we do note that this effect does not inhibit enhanced structure of the solvent, as this happens in the case of OH^-.

Bonding within the $OH^{\bullet}\cdot(H_2O)_4$ Solvation Complex. The flat arrangement of the three water molecules (W1, W2, and W3) around the $OH^{\bullet}$ radical suggests that the central O* atom is in an sp^2 hybridization state with the two lone pair hybrid orbitals oriented toward the W2 and W3 molecules and taking part in hydrogen bonds as H-bond acceptors. The p_π molecular orbital (MO) is then perpendicular to this plane and points toward the W4 water molecule. From projected density of states and spin-density data (difference between up and down spin density) it can be shown that the p_π orbital is the singly occupied molecular orbital of the hydroxyl radical in this solvated state.

The short distance between the central O* atom and the W4 water molecule as well as the stability of this configuration suggest possible direct interaction between the two oxygens. To test this, for a selected configuration from the MD run we calculated the projected density of the Kohn−Sham electron states on local (atomic) p projectors centered in either of the oxygen atoms of the OH or W4. The p projectors are oriented along the axes connecting the two atoms; i.e., they coincide with the p_π MO of the $OH^{\bullet}$ and the p_π ($1b_1$) MO of W4. The data presented in Figure 6 reveal the formation of a three-electron two-centered σ bond between the two oxygens. Of the resulting four spin-polarized molecular orbitals, three are occupied (two bonding and one antibonding) and one is unoccupied (antibonding).

The relatively large split in the eigenvalues of more than 2 eV suggests a strong interaction. It has been shown, however, that the bond energy using the BLYP-DFT method is relatively small and comparable to the energy of a hydrogen bond (see, for example, ref 1 and references therein). This is because one of the occupied molecular orbitals is antibonding and destabilizes the system. Nevertheless, it has to be stressed that the singly occupied p_π MO of the hydroxyl radical is tied down in this hemibond, and this may have consequences for the activity of the $OH^{\bullet}$ and the process of the $OH^{\bullet}$ diffusion via hydrogen exchange reaction.

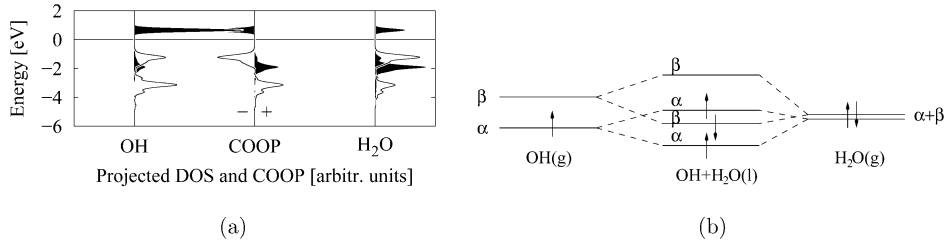

Figure 6. Formation of a hemibond between OH• and a water molecule. (a) Projected density of states and COOP. Solid lines correspond to the α electron states, filled curves correspond to the β electron states. The COOP data indicates the character of the corresponding state and is positive if the state is bonding for the interaction between the OH• (left) and H_2O (right) and negative if the state is antibonding. (b) Schematic representation of the formation of the hemibond.

Diffusion and Activity of the Hydroxyl Radical in Liquid Water. The structure and electronic properties of the solvated hydroxyl radical are of crucial importance for understanding the oxidation processes involving OH• as an intermediate. If the unpaired electron in the p_π molecular orbital of the OH• is tied down in a hemibond, this effectively inhibits the oxidative properties of the radical. The supposed mechanism of diffusion of OH· in liquid water via a hydrogen exchange reaction can also be no longer efficiently operative.

It has to be pointed out that the diffusion mechanisms of hydroxyl radical and hydroxide ion in water are fundamentally very different. While for the OH^- the diffusion takes place via a *proton* exchange reaction with hydrating H_2O molecules, in the case of the OH• radical the analogous process would be *hydrogen* exchange. In either case, the necessary condition for the reaction to take place is that the hydrating H_2O taking part in the exchange process should have its OH bond pointing toward the hydroxide, respectively hydroxyl species. As was shown by Tuckerman et al.,[23] OH^- forms (in its active state) three hydrogen bonds satisfying this condition. On the contrary, in the case of the OH• radical only two bonds (those of W2 and W3, Figure 5) point toward the OH, but neither of them can take part in a *hydrogen* exchange reaction. A hydrogen exchange reaction, which involves the transfer of a proton and an electron, could take place if the associated water molecule forms a H-bond via the singly occupied p_π MO of the radical. As seen from the current simulations, this event never occurs during the MD run because the p_π MO takes part in a hemibond with W4.

It is interesting to compare our results to previous studies comparing BLYP-DFT results with high-level ab initio calculations[1,5−9] for small gas-phase clusters of OH• with a few water molecules. These cluster calculations raise two issues. In the first place, they do not show the solvation pattern depicted in our Figure 5. For instance, with four or five water molecules surrounding OH• in the gas-phase cluster, the structure of Figure 5 is not formed, but with either BLYP or MP2 the OH• forms only two or three hydrogen bonds to neigboring water molecules and no hemibond.[1] So if the solvent molecules from the bulk liquid water surrounding the complex were not present, the structure of Figure 5 would rearrange, the hydrating water molecules W1, W2, W3, and W4 forming hydrogen bonds among themselves. Such rearrangement of the molecules would result in the destruction of the hydration complex of Figure 5. This means that although the $OH^{\bullet}\cdot(H_2O)_4$ hydration complex does not possess an identifiable second coordination shell (see above), the presence of the solvent is still quite essential for the local structure of the hydrated OH· and its stability over time. In the liquid phase the "unsaturated" hydrogen bonds of the complexing H_2O can be realized with water molecules from the second coordination shell. This can explain the differences between the current periodic DFT simulation and the previous cluster DFT data.[1]

In the second place, calculations on small systems have shown that the BLYP density functional overestimates the strength of the three-electron two-center hemibonds.[1,7−9,28] However, on the basis of cluster calculations it has been argued that the differences between the two methods (DFT and high-level ab initio) diminish with increasing size of the system, particularly the number of water molecules.[1] For instance, in the largest gas-phase cluster considered, with five H_2O molecules, BLYP and MP2 yield very similar structures and hydration energies. However, this is not yet conclusive evidence that in very large clusters, or in bulk water, the difference between BLYP and MP2 would also be negligible. In fact, in small clusters the geometry of the cluster is dictated by the requirement of forming as many hydrogen bonds as possible, which yields the energetically most favorable configuration. As long as no hemibond is present, which is the case in the gas-phase clusters with four or five water molecules surrounding OH•, there will not be a marked difference between BLYP and MP2, since the H-bonds in BLYP and MP2 are very similar. However, it is still possible that the BLYP result would reflect the overbinding of the hemibond compared to the MP2, if a sufficiently large cluster is being used, which has a water molecule hemibonded to the OH· radical and embedded in hydration shells stabilizing the configuration. At this point, we feel the bulk simulations have revealed a solvent coordination of the OH• radical (see Figure 5) which is quite plausible as far as the hydrogen bond donor role of OH• to W1 and its hydrogen bond acceptor role with respect to W2 and W3 are concerned. As for the coordination of W4 to OH•, it is clear that the hemibonded structure plays an important role. To what extent, the BLYP functional overestimates the strength of this bond in the case of the actual situation in the solvent (the structure of Figure 5 with surrounding solvent molecules) is a question which requires further examination. We are undertaking such investigations, using extensive application of post-Hartree−Fock ab initio methods to relevant OH•−water clusters.

Conclusions

The presented results of Car−Parrinello molecular dynamics of OH• in liquid water reveal the formation of a relatively stable first solvation shell of the radical. The OH• species are bound to three neighboring water molecules via hydrogen bonds. The unpaired electron of the radical is tied up in a three-electron, two-center hemibond with a fourth neighboring water molecule. This suggests that the supposed diffusion mechanism of OH• via a hydrogen exchange reaction in these conditions may not be efficiently operative. The extent of this effect may be partially overestimated by the tendency of the BLYP exchange-correlation density functional to overestimate the strength of the

hemibond. Further examination of the structural properties and bond strength in this system in comparison with post-Hartree−Fock calculations are therefore necessary and are currently underway. With such information available it will be possible to construct an accurate functional for the hemibonding. Constrained dynamics along a reaction coordinate from the water molecule hemibonded to H-bonded via the singly occupied π MO of the radical would then enable crucial information on what should be the first step in the difusion mechanism by H abstraction from the water molecule.

Acknowledgment. We acknowledge financial support from The Netherlands' National Research School Combination "Catalysis by Design" (NRSC-C).

References and Notes

(1) Hamad, S.; Lago, S.; Mejìas, J. A. *J. Phys. Chem. A* **2002**, *106*, 9104.
(2) Fenton, H. J. H. *J. Chem. Soc*. **1894**, *65*, 899.
(3) Ensing, B.; Baerends, E. J. *J. Phys. Chem. A* **2002**, *106*, 7902.
(4) Ensing, B.; Buda, F.; Blochl, P. E.; Baerends, E. J. *Phys. Chem. Chem. Phys*. **2002**, *4*, 3619.
(5) Kim, K. S.; Kim, H. S.; Jang, J. H.; Kim, H. S.; Mhin, B.-J.; Xie, Y.; Schaefer, H. F., III. *J. Chem. Phys*. **1991**, *94*, 2057.
(6) Xie, Y.; Schaefer, H. F., III. *J. Chem. Phys*. **1993**, *98*, 8829.
(7) Wang, B.; Hou, H.; Gu, Y. *Chem. Phys. Lett*. **1999**, *303*, 96.
(8) Zhou, Z.; Qu, Y.; Fu, A.; Du, B.; He, F.; Gao, H. *Int. J. Quantum Chem*. **2002**, *89*, 550.
(9) Cabral do Couto, P.; Guedes, R. C.; Costa Cabral, B. J.; Martinho Simões, J. A. *J. Chem. Phys*. **2003**, *119*, 7344.
(10) Nanayakkara, A. A.; Balint-Kurti, G. G.; Williams, I. H. *J. Phys. Chem*. **1992**, *96*, 3662.
(11) Dubey, M. K.; Mohrschladt, R.; Donahue, N. M.; Anderson, J. G. *J. Phys. Chem. A* **1997**, *101*, 1494.
(12) Hand, M. R.; Rodriquez, C. F.; Williams, I. H.; Balint-Kurti, G. G. *J. Phys. Chem. A* **1998**, *102*, 5958.
(13) Hohenberg, P.; Kohn, W. *Phys. Rev*. **1964**, *136*, B864.
(14) Kohn, W.; Sham, L. J. *Phys. Rev*. **1965**, *140*, A1133.
(15) Car, R.; Parrinello, M. *Phys. Rev. Lett*. **1985**, *55*, 2471.
(16) Laasonen, K.; Sprik, M.; Parrinello, M. *J. Chem. Phys*. **1993**, *99*, 9080.
(17) Sprik, M.; Hutter, J.; Parrinello, M. *J. Chem. Phys*. **1996**, *105*, 1142.
(18) Silvestrelli, P. L.; Bernasconi, M.; Parrinello, M. *Chem. Phys. Lett*. **1997**, *277*, 478.
(19) Vassilev, P.; Hartnig, C.; Koper, M. T. M.; Frechard, F.; van Santen, R. A. *J. Chem. Phys*. **2001**, *115*, 9815.
(20) Marx, D.; Tuckerman, M. E.; Hutter, J.; Parrinello, M. *Nature* **1999**, *397*, 601.
(21) Geissler, P. L.; Dellago, C.; Chandler, D.; Hutter, J.; Parrinello, M. *Chem. Phys. Lett*. **2000**, *321*, 225.
(22) Tuckerman, M.; Laasonen, K.; Sprik, M.; Parrinello, M. *J. Chem. Phys*. **1995**, *103*, 150.
(23) Tuckerman, M. E.; Marx, D.; Parrinello, M. *Nature* **2002**, *417*, 925.
(24) Trout, B. L.; Parrinello, M. *J. Phys. Chem. B* **1999**, *103*, 7340.
(25) Becke, A. D. *Phys. Rev. A* **1988**, *38*, 3098.
(26) Lee, C.; Yang, W.; Parr, R. G. *Phys. Rev. B* **1988**, *37*, 785.
(27) Bickelhaupt, F. M.; Diefenbach, A.; de Visser, S. P.; de Koning, L. J.; Nibbering, N. M. M. *J. Phys. Chem. A* **1998**, *102*, 9549.
(28) Sodupe, M.; Bertran, J.; Rodriguez-Santiago, L.; Baerends, E. J. *J. Phys. Chem. A* **1999**, *103*, 166.
(29) Blöchl, P. E. *Phys. Rev. B* **1994**, *50*, 17953.